Crack Resistance Behaviour of Pressure Die Cast Magnesium Alloys

D. Regener and G. Dietze

Institute of Materials Engineering and Materials Testing
Otto-von-Guericke-University Magdeburg, Germany
PSF 4120, D-39016 Magdeburg

ABSTRACT: *The increasing use of pressure die cast magnesium alloys for the manufacturing of automotive components requires materials values, which describe completely the mechanical behaviour. Present, there is a lack of data, especially for the design process of safety relevant components. Therefore, fracture mechanics investigations were carried out to assess the crack resistance of the alloys AZ91, AM50 and AE42 on the basis of the multispecimen test method. The investigations occurred on SENB- and CT-specimens taken from plate-like components of the same dimensions.*
The results clearly reveal the correlation between crack resistance and microstructure concerning mainly the influence of the concentration and distribution of intermetallic phases. Because of the cast-induced defects like microshrinkage and gas inclusion the good intrinsic properties of the alloys are not exploited.

INTRODUCTION

In the recent years the interest in applying magnesium alloys is rapidly grown. The low weight, the good castability and manufacturability as well as the high specific strength distinguish magnesium alloys as excellent lightweight materials. The majority of the global growth in the usage of magnesium alloys is related to die castings for automobile applications [1-4]. In order to obtain a high property level of the material and to ensure the functionality of the product, special pressure die cast alloys on the basis of the systems Mg-Al-Zn, Mg-Al-Mn, Mg-Al-Si and Mg-Al-RE have been developed. However, the exploitation of the materials potential depends essentially on the transformation of the good intrinsic properties of the material in the behaviour of the cast component [5].

Present, the manufacturing of sound die cast parts can yet not be ensured. Numerous defects like pores and microcracks often lead to a reduction of strength and ductility [6-9]. However, because of the lack of reliable data it is not possible to assess the damage tolerance of the used material in safety-related components. Therefore, the aim of this paper is to investigate the crack resistance of the die cast magnesium alloys AZ91, AM50 and AE42 as well as to reveal the microstructural origins of the different materials behaviour.

MATERIALS CHARACTERISATION AND EXPERIMENTAL

For the investigations plate-like components from the called alloys with the dimensions of 200 x 75 x 10 mm were cast on a cold chamber die-casting machine. The chemical composition of the alloys is presented in Table 1. Except the too low Mn-values of the alloys AZ91 and AM50 and the too low Al-value in AM50 the contents of the elements are in accordance with the recommendations [10].

TABLE 1: Chemical composition of alloys investigated

Alloy	% Al	% Mn	% Zn	% Si	% Cu	% Ni	% Fe	% RE
AZ91	9.3	0.12	0.79	0.02	0.0007	0.0006	0.0046	
AM50	4.1	0.24	<0.0001	0.006	<0.0002	0.0004	0.0020	
AE42	4.2	0.18	0.013	0.002	0.0120	0.0009	0.0023	2.614

The mechanical values R_m, E and A (Table 2) are based on the testing of proportional flat tensile specimens taken from the plates (gauge length: 55 mm, thickness: 10 mm) as well as of separately die cast proportional flat test bars (gauge length: 55 mm, thickness: 5 mm).

TABLE 2: Mechanical properties

Alloy	R_m (N/mm^2)	A (%)	E (GPa)	K (J)
AZ91	175 (208)*	1.3 (1.7)	42 (48)	2.5
AM50	161 (218)	2.7 (6.6)	50 (48)	12.9
AE42	141 (192)	1.0 (4.6)	46 (46)	7.4

* Values obtained of the separately cast specimens in brackets

It is obvious that the specimens taken from the plates do not reach the ultimate strength R_m and the strain at rupture A of the separately cast specimens. The lower strength of the component related specimens is mainly attributed to their greater thickness. This results in a coarse grain structure through the section and a low fine grained marginal layer. The decreased strain values are due to the higher porosity in the thicker wall. With respect to the different materials the component related specimens from the alloy AZ91 show the highest strength, whereas the specimens from the alloy AM50 show the highest strain at rupture. The elastic modulus values of the alloys achieve the same order of magnitude for the both specimen series. However, the scattering of the values is broader using the component related specimens.

The results of impact tests carried out on unnotched Charpy specimens in a pendulum impact machine (maximum of impact energy = 20.3 J) already reveal a distinct toughness of the alloys. In accordance with the data in [10] the lowest average K-value is found in AZ91, the highest one in AM50.

The assessment of the crack resistance behaviour under static loading occurred on the basis of the multispecimen test method using fatigue precracked SENB- (10 x 10 x 55 mm) and CT-specimens (W =20 mm, H = 24 mm, 9.35 mm) taken from the plates. The stable crack extension Δa was measured on the fracture surface after heat tinting at 350 °C/2h (AZ91) and at 430 °C/2h (AM50 and AE42).

For the investigation of the microstructure the specimens were prepared by wet grinding until 4000 mesh silicon carbide paper, followed by polishing with finally 1 µm diamond paste and etching with 3 % alcoholic nitric acid.

RESULTS AND DISCUSSION

Microstructure

The metallographic investigation of the alloy AZ91 reveals a cored dendritic microstructure through the whole plate thickness (Fig. 1a).

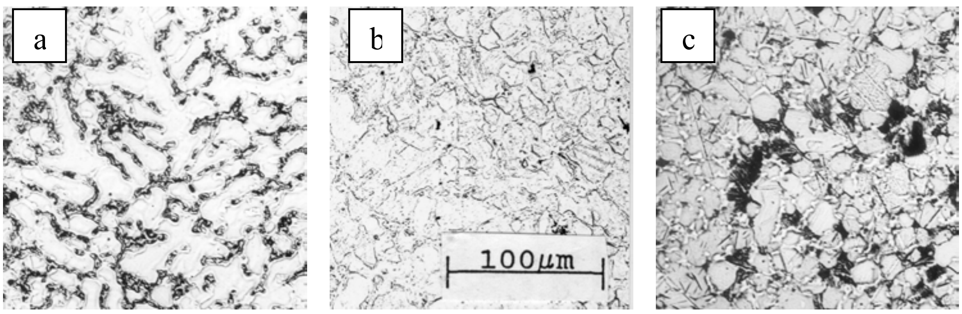

Figure 1: Microstructure of the investigated alloys AZ91 (a), AM50 (b) and AE42 (c)

The dendrites are formed by the primary α-Mg solid solution grains surrounded by a divorced eutectic, in which the intermetallic β-phase $Mg_{17}Al_{12}$ is embedded in α-Mg that is richer in Al than the primary α-Mg. In the alloy AM50 a similar microstructure is found (Fig. 1b). However, due to the reduced Al-content the volume of the divorced eutectic is less resulting in a low content of β-phase in an isolated form.

The microstructure of alloy AE42 shows a globular α-matrix with coring as well as a lamellar eutectic with different phases of the Al-RE- and Mg-Al-type (Fig. 1c).

Concerning the soundness the highest porosity due to microshrinkage or gas inclusion is present in the plates from the alloy AE42. The reason is the reduced castability of this alloy.

Crack Resistance Behaviour

Selected load-displacement-curves obtained from SENB-specimens (Fig. 2) provide information about the energy absorption of the alloys.

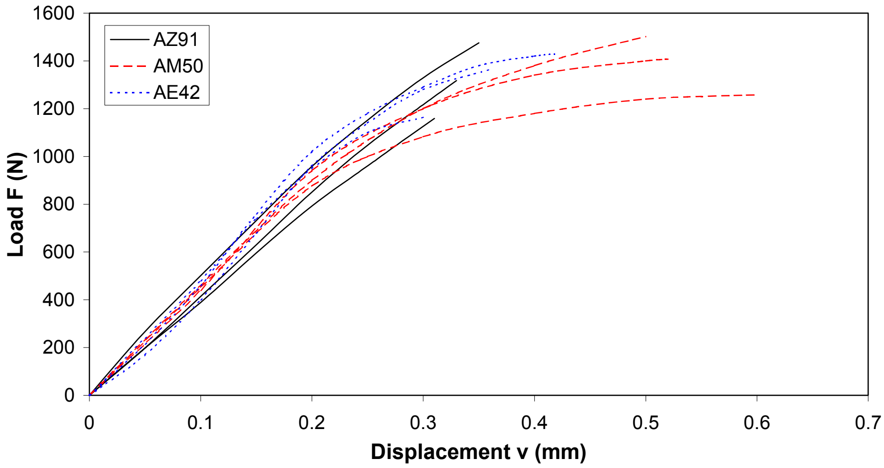

Figure 2: Load-displacement curves obtained from SENB-specimens

The best energy absorption capability is observed for the alloy AM50 owing to a high plastic part of deformation. In contrast, the displacement values of the AZ91 specimens are essentially based on an elastic deformation. The alloy AE42 takes in its energy absorption capability an intermediate position. The more or less strong variation of the curves arises from the differences of the fatigue crack geometry and especially from cast induced defects at the crack front. This behaviour of the alloys is confirmed by investigations on CT-specimens and is also in accordance with the tendency of the impact energies from the Charpy test as well as of the strain values at rupture from the tensile tests.

The experimental determination of crack resistance curves J-Δa of pressure die cast magnesium alloys proves difficult. Though the heat tinting leads to a marking of stable crack growth, there are problems to recognise the boundary between the fatigue crack and stable crack. In addition, cast induced defects present in the region of the stable crack impede the precise measurement. Fig. 3 shows examples of the stable crack growth in CT-specimens from the investigated alloys.

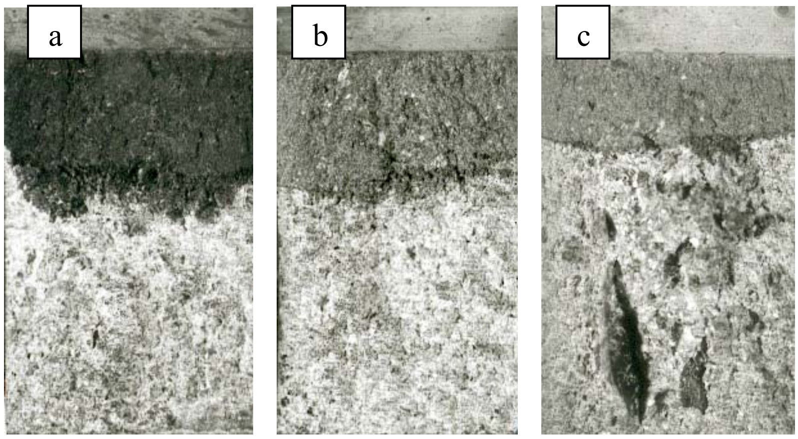

Figure 3: Macroscopic fracture surfaces of CT-specimens from AZ91 (a), AM50 (b) and AE42 (c)

The appearance of the crack front often reveals an irregular stable crack growth influenced by different microstructural phases and cast induced defects. The relative fast crack growth observed in the alloy AZ91 is attributed to the high content of the brittle intermetallic phase $Mg_{17}Al_{12}$ at the grain boundaries. Frequent disturbances of the crack growth front are observed in specimens from the alloy AE42 because of the high volume porosity.

The experimentally determined J-Δa-pairs result in the crack resistance curves using a power function of the type $J = A \cdot \Delta a^D$ for the value fitting.

The curves obtained from SENB-specimens (Fig. 4) reflect a relatively low crack resistance regarding not only the crack initiation but also the tearing. To characterise the sensitivity of the material to crack initiation, the crack resistance $J_{0.2}$ is used. The determination of J_i-values is not possible, because a remarkable blunting of the crack tip does not occur. The most favourable $J_{0.2}$-value is obtained for the alloy AM50 (Table 3), the lowest one for the alloy AZ91. This means that in presence of internal defects and incipient cracks the behaviour of components from AZ91 is less damage tolerant than that of components made from AM50 and AE42. The cause is the different microstructure of the alloys, in which the concentration and distribution of the intermetallic phases play an important role. Regarding the alloys AZ91 and AM50 the differences are especially attributed to the concentration of the phase $Mg_{17}Al_{12}$ at the grain boundaries, which is high in the alloy AZ91 and low in the alloy AM50.

The resistance to crack tearing characterised by the slope of the J versus Δa curves ΔJ/Δa for a comparable crack growth beyond 0.2 mm is hardly different between AZ91 and AM50. The unacceptable resistance of the AE42 specimens is not attributed to the intrinsic properties of the alloy, but to the large number of internal defects.

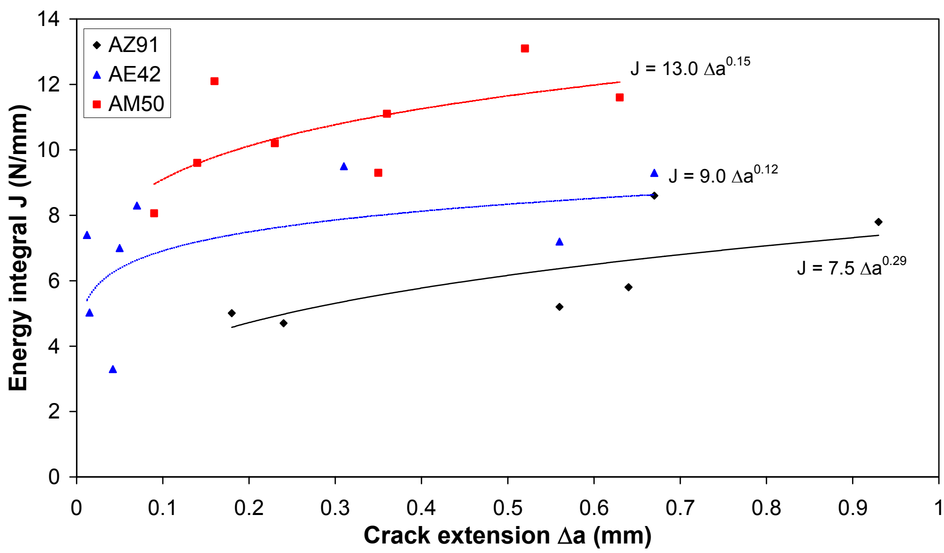

Figure 4: Crack resistance curves obtained from SENB-specimens

In comparison, the J-Δa-curves obtained from CT-specimens (Fig. 5, Table 3) are changed to higher values due to the geometrical influence. Regarding the different alloys the curves confirm the same tendency of the crack resistance behaviour. Unfortunately, up to now comparable investigations are not found in the literature. However, previous own fracture toughness tests carried out on specimens of other castings show the best values for the alloy AE42 [11]. These differences reveal clearly the special influence of the cast process.

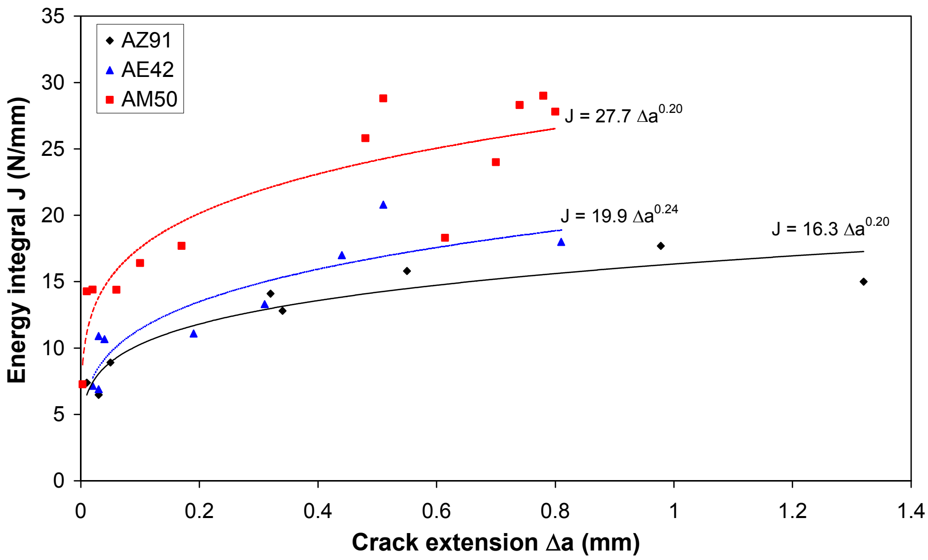

Figure 5: Crack resistance curves obtained from CT-specimens

TABLE 3: Crack initiation values $J_{0.2}$

Alloy	$J_{0.2}$ (N/mm)		$\Delta J/\Delta a$	
	SENB	CT	SENB	CT
AZ91	4.7	11.8	4.4	7.3
AE42	7.4	13.5	3.3	10.3
AM50	10.2	20.1	4.5	12.3

CONCLUSIONS

The investigations of the alloys AZ91, AM50 and AE42 show a dendritic microstructure and reveal a different concentration and distribution of intermetallic phases in dependence on the composition as well as a different cast-induced porosity. These differences have a distinct effect on the crack resistance behaviour. The alloy AZ91, in which the brittle intermetallic phase $Mg_{17}Al_{12}$ is strongly concentrated at the grain boundaries, shows the lowest resistance to crack initiation and propagation. In opposite, the alloy AM50 containing a low amount of $Mg_{17}Al_{12}$ achieves the highest resistance. Because of the above-average number of internal defects the crack growth of the alloy AE42 does not reflect its good intrinsic properties. In order to exploit the intrinsic properties of all investigated alloys comprehensively, the manufacture-induced defects have to be reduced by improvement of the casting technology.

ACKNOWLEDGEMENT

The authors like to express their gratitude to the Kultusministerium des Landes Sachsen-Anhalt for the financial support of this research work.

REFERENCES

1. Albright, D.L., Ruden, T., Davis, J. (1992) *Light Metal Age* **50**, 28.
2. Mezoff, J.G. (1992). In: *Magnesium in automobiles,* pp. 1-14, International Magnesium Association, Warrendale, Pa., SAE-SP 800417.
3. Haldenwanger, H.-G., Rösch, R. (1998) *Gießerei-Praxis* Nr. 2, 62.
4. Mordike, B.L., Ebert, T. (2001) *Materials Science and Engineering* **A 302**, 37.
5. Aune, T.K., Westengen, H., Albright, D. (2001) *Magnesium* No. 1, 25.
6. Sasaki, H., Adachi, M., Sakamoto, T., Takimoto, A. (1997) *Gießerei-Praxis* Nr. 15/16, 341.
7. Dunlop, O.L., Sequeira, W.P., Dargusch, M.S., Song, C., Atrens, A., Kittel, T., St. John, D.H., Dahie, A.K., Murray, M. (1999) *Gießerei-Praxis* Nr. 9, 453.
8. Kinzler, T., Klein, F. (1998) *Metall* **52**, 716.
9. Zheng liu, Lihe Chen, Huijie Zhao, Yue Wang, Zhongguang Wang, Klein, F. (2000) *Metall* **54**, 122.
10. Datenblatt Magnesiumdruckgusslegierungen. Hydro Magnesium 06/00
11. Schick, E., Regener, D. (2000). In: *ECF13*, 6-9 Sept. 2000, San Sebastian, Spain